A study on the environmental state of the Caribbean Sea in relation to the rapid intensification of tropical cyclone Matthew

T. Cömert, C. A. Katsman, C. G. van der Boog

Department of Hydraulic Engineering, Delft University of Technology, Delft, Netherlands

Abstract

Tropical cyclones have the ability to very quickly increase in strength. This process is called rapid intensification and as a result, tropical cyclones can transform into hurricanes. Rapid intensification is related to the availability of heat and the amount of negative feedback of the ocean on the tropical cyclone. Negative feedback results in the weakening of the tropical cyclone. Cyclones passing over a warm ocean anomaly have access to more heat and due to the relatively high temperatures, the amount of negative feedback is reduced considerably. A necessary condition for rapid intensification is therefore the presence of a warm ocean anomaly, often being warm core eddies. This paper relates the rapid intensification of tropical cyclone Matthew to the presence of warm core eddies in the track of Matthew. Results show that there is no extensive evidence found for the presence of a warm core eddy before rapid intensification took place. Although maps of the sea surface height and sea surface temperature indicate the possible existence of a warm core eddy, surface velocities do not show the characteristic rotation flow of an eddy. The enthalpy flux is considerably large just before the rapid intensification of Matthew indicating that the negative feedback by the ocean is reduced and heat is available for transport. The rapid intensification of Matthew might be linked to other physical mechanisms that have been overlooked. Possible mechanisms identified are the Amazon-Orinoco river plume and La Niña. Further studies on the rapid intensification of tropical cyclone Matthew should therefore take into account these mechanisms and study their influence on rapid intensification.

Keywords: Caribbean Sea, Tropical Cyclones, Warm Core Eddies, Air-Sea Interaction, Air-Sea Fluxes, Rapid Intensification, Negative Feedback

1. Introduction

Research has shown that the damages caused by hurricanes will continue to increase in the future. The growing population along coastal areas contributes to this (Creel, 2003). Furthermore, the rapid intensification of tropical cyclones to hurricanes is underestimated - or even missing - in analyses, leading to incomplete evacuations (Goldenberg et al., 2001). Studies (Blake et al., 2007; Pielke Jr et al., 2008; Blake et al., 2008; Malmstadt et al., 2009) show the adverse impact by hurricanes on the economical and social structures of the affected areas. Combined with global warming, studies in hurricane development are essential in mitigating the consequences.

The rapid intensification of tropical cyclones into hurricanes is one of the main focuses of hurricane development research. Tropical cyclones are low-pressure systems over (sub)tropical waters with organized convection and wind circulation (Holland, 1993). In the Northern and Southern Hemisphere, tropical cyclones are cyclonic. Rapid intensification is defined as the rapid deepening of tropical cyclones by 42 *mb* in 24H (Holliday and Thompson, 1979) or a 15 $m/s\ day^{-1}$ increase in the maximum surface wind velocity (Kaplan and DeMaria, 2003). The general result of rapid intensification is a stronger tropical cyclone. When the intensification is very strong, the tropical cyclone can develop into a hurricane (Saffir-Simpson tropical cyclone scale (Simpson and Saffir, 1974)).

The primary source in the rapid intensification period is the interaction between air and sea. Previous research (Hong et al., 2000; Lin et al., 2009, amongst others) on rapid intensification periods concentrates on (warm)

Email address: t.comert@student.tudelft.nl (T. Cömert)

ocean anomalies, mostly ocean mesoscale eddies. The general theory is that when tropical cyclones pass over a warm core eddy, which carries water with more heat relative to its surrounding waters, it absorbs the heat of the eddy resulting in rapid intensification (Hong et al., 2000). Case studies are widely used to assess when and how tropical cyclones develop into hurricanes during the rapid intensification period. There is still a gap in knowledge that leads to difficulties in predicting the rapid intensification periods of tropical cyclones (Kaplan et al., 2010), but with these case studies, more knowledge regarding relevant physical mechanisms is gained.

Hurricane Matthew (2016) experienced a rapid intensification from tropical cyclone to major hurricane. Emerging as a tropical wave at the west coast of Africa on 23 September, Matthew moved within three days across the tropical Atlantic and reached its tropical cyclone status on 28 September, west-northwest of Barbados (Figure 1) (Stewart, 2017). The next few days, Matthew moved into the Caribbean Sea and reached hurricane status on 29 September. Rapid intensification took place from 30 September till 1 October. During this period, the pressure decreased from 987 mb to 942 mb and wind velocities increased from 36 m/s to 75 m/s (Stewart, 2017). After undergoing a rapid intensification, Matthew continued its path (Figure 1) through the Caribbean Sea and ultimately lost its tropical cyclone status on 9 October near North Carolina, USA (Stewart, 2017).

Forecast models have failed in predicting the rapid intensification of Matthew, while the performance in predicting the genesis and further stage after rapid intensification was rather good (Stewart, 2017). Responsible for 585 direct deaths and billions of dollars damage, Matthew is one of the more destructive hurricanes in recent history (Blake et al., 2018).

Although the impact of Hurricane Matthew is indisputable, an analysis of its rapid intensification is missing. The rapid intensification may have been initiated by a warm core eddy in the Caribbean Sea. Previous research (Rudzin et al., 2017) indicates that warm core eddies in the Caribbean Sea could influence air-sea processes, e.g. during the passing by of tropical cyclones.

The aim of this study is to look at the occurrence and positioning of warm core eddies in the Caribbean Sea in relation to the rapid intensification period of tropical cyclone Matthew. In order to assess this, the following research question is answered:

Does the location and time of the rapid intensification period of Hurricane Matthew coincide with the occurrence of Warm Core Eddies in the area of interest within the Caribbean Sea?

To answer this research question, the following approach is applied:

1. Literature study, primarily aimed at previous case studies, to identify the relevant parameters of warm core eddies and tropical cyclones
2. Data analysis of physical parameters during Matthew's passage through the Caribbean Sea
3. Comparison between locations of warm core eddies and rapid intensification of Matthew, and analysis of relevant parameters following from the literature study

Section 2 of this paper provides an overview of the known theory regarding eddies and the rapid intensification of tropical cyclones. Case studies of previous tropical cyclones are summarized and several key elements that need attention in the data analysis are explained. The datasets used for the data analysis are briefly described. The results and discussion are stated in Section 3 and Section 4 focuses on the conclusion and recommendations for future research.

2. Scientific Background in the Caribbean Sea

In Section 2.1, theoretical concepts of intensification and weakening of tropical cyclones are shown. Several characteristics of the Caribbean Sea and its warm core eddies are summarized (Section 2.2), and results of some case studies for tropical cyclones rapidly intensifying into hurricanes are analysed (Section 2.3). In the end, an overview of the details regarding the datasets used in the data analysis is given (Section 2.4).

2.1. Intensification and Weakening of Tropical Cyclones

Tropical cyclones only form at warm waters near the equator (more specifically tropical zones). When warm air at the sea surface rises up, the air pressure at the sea surface lowers. As a result, air from surrounding areas flows in to compensate for the lower air pressure and also becomes warmer, after which the cycle repeats. Eventually, the system will spin and a tropical cyclone is initiated. The ocean thus provides the heat to warm

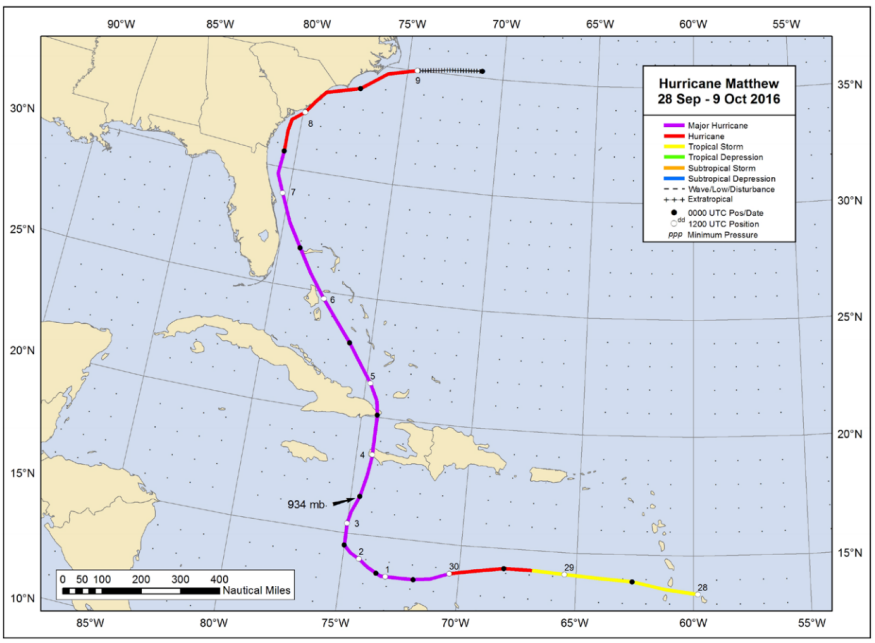

Fig. 1 *Best track positions for Hurricane Matthew, color of lines indicate the type of storm and dates are given as numbers next to the track. Figure taken from Stewart (2017).*

the air and this feedback leads to the start and growth of tropical cyclones. Depending on the magnitudes of this heat flux, the tropical cyclone will have a certain strength.

The air-sea interaction between tropical cyclones and the ocean is thus an important physical mechanism. This is also important in cases of intensification and weakening of tropical cyclones. Intensification of the tropical cyclone takes place when the heat flux provided by the ocean is larger than the intake of heat by the tropical cyclone. When this holds, the tropical cyclone will intensify until the heat flux is enough to maintain the strength of the tropical cyclone.

Weakening of tropical cyclones is another possibility. The general theory states that tropical cyclones passing over the ocean cool the upper ocean layer due to vertical shear-induced mixing and upwelling. In turn, heat fluxes at the ocean surface will change, resulting in an decreased flux of (ocean) heat to the tropical cyclone. This leads to the weakening of the intensity of the storm (Hong et al., 2000).

A more mathematical approach is suggested by Emanuel (1986). The proposed axisymmetric model explains a large part of the air-sea interaction. Although highly idealized, the purpose of this steady-state model is to show the interplay between physical processes.

The air-sea interface is modelled by a well-mixed surface boundary layer with a thermal wind balance flow above this layer (Emanuel, 1986). With some derivations, a relationship between central surface pressure and the increase in surface relative humidity between the core and the ambient environment is found (Emanuel, 1986). Emanuel (1986) explains this relationship in the following manner:

> A transfer of heat above and beyond that associated with isothermal expansion is needed to sustain a tropical cyclone. This extra-isothermal transport is reflected by an inward increase of relative humidity.

This means that whenever there is a difference in inflow and outflow of heat or vapor content, the surface pressure becomes smaller. Emanuel (1986) shows that the surface pressure is very sensitive to surface air temperature. Ultimately, the steady-state model resembles a Carnot heat engine in which latent and sensible heat fluxes are mainly responsible for the heat source extracted from the ocean (Emanuel, 1986). The disadvantage of this mathematical approach is the amount of assumptions that neglect key elements within tropical cyclones, such as the dynamics of the eye of the tropical cyclone (Emanuel, 1986).

The ocean heat content proves to be a stable measure for the amount of heat contained in the ocean. Ocean heat content is defined as:

$$H = \rho c_p \int_{h_1}^{h_2} T(z)dz \quad (1)$$

where H is the amount of ocean heat content $[J/m^2]$, ρ the seawater density $[kg/m^3]$, c_p the specific heat of water $[J/kgK]$, h_1 and h_2 the integration boundary depths $[m]$ and $T(z)$ the vertical temperature profile $[K]$.

In conclusion, tropical cyclones affect the ocean mixed layer and depending on the amount of induced cooling, intensification can be initiated. Intensification is reached by heat transport through the sensible and latent heat fluxes. Rapid intensification depends on the increase of strength (see Section 1 for definition).

2.2. Warm Core Ocean Mesoscale Eddies

Warm core eddies (anticyclonic) are warmer relative to their surrounding waters, resulting in water flowing outwards. In the Northern Hemisphere, the direction of rotation due to the Coriolis force is to the right, leading to a clockwise flow in the eddy. Due to the difference in properties of warm and cold water, warm core eddies possess a positive sea surface height difference. Warm water takes more space than cold water due to its expansion, resulting in sea surface height anomalies. Cold core eddies are exactly the opposite of warm core eddies and thus show a anticlockwise rotation (cyclonic). Observational studies (Richardson, 2005) show that in the Caribbean Sea, an almost equal amount of cyclonic and anticyclonic eddies are present, thus in relation with rapid intensification not all eddies will be relevant.

Mesoscale eddies have a diameter of a few hundred kilometers. This substantial size is explained by the Rossby radius of deformation. Length scales near the equator, at which the Coriolis force has an impact, are much larger than at high latitude zones. Measurements by Richardson (2005) show that anticyclonic eddies have diameters of 200 km, whereas numerical simulations show widths between 200 and 500 km (Jouanno et al., 2008). The size of these eddies is almost equal to the extent of the Caribbean Sea and the eddies have important traits, such as their influence on the deep mean circulation as well as vorticity balances. Mesoscale eddies also show an impact on ecology (Lobel and Robinson, 1986), emphasizing their important role in ocean as well as ecological dynamics.

Mesoscale eddies have an energetic profile and exist for several months. Numerical model studies (Holland and Lin, 1975) show that the potential energy of the mean flow is transferred to the separated eddies. Jouanno et al. (2008) show that eddies propagating westwards in the Caribbean Sea intensify with respect to the eddy kinetic energy. Mesoscale eddies can also be influenced by other physical phenomena. In the Caribbean Sea, the Amazon-Orinoco river plume is an important physical parameter influencing eddies with respect to temperature and salinity. Ongoing research focuses on the changes in hydrodynamics of eddies due to this river plume and other physical phenomena (van der Boog, 2018). There is not a clear answer to the lifetime of eddies in the Caribbean Sea. Numerical simulations by Jouanno et al. (2008) suggest the time scale, at which the eddies are present, is between 50 and 110 days. This is almost equal to the results by Carton et al. (1999), who indicated 3 month time scales.

In the Caribbean Sea, mesoscale eddy studies show that eddies can extend to depths of a 1000 m (Corredor et al., 2011) and they can originate from in- and outside the Caribbean Sea. Buoy observations by Molinari et al. (1981) suggest that the source of the mesoscale variability might be due to the rises and ridges of the Caribbean Sea. This is only true if the flow is in the same direction from the sea surface to the ocean floor (Molinari et al., 1981). Data analyses by Richardson (2005) suggest a formation rate of 8-12 anticyclones per year, with most of the eddies forming between September and November. A possible source of these eddies might be the collision between the North Brazilian Current rings and the Lesser Antilles (Richardson, 2005). Altimetry data also suggest eddies originating in the Venezuelan Basin (Andrade and Barton, 2000).

Numerical simulations by Carton et al. (1999) show that the eddies act on almost a 250 km spatial scale, progressing westwards with speeds of roughly 12 cm/s and crossing the Caribbean basin in approximately 180 days. The vertical structure of eddies show that their influence is felt far underneath the sea surface as they primarily hold warmer water than their surroundings. Surveys by Rudzin et al. (2017) prove that the isothermal layer depth is much deeper in the eddies than the background flow in the Caribbean Sea. Furthermore, the 26°C isotherm depth is deeper in the eddies, suggesting a larger ocean heat content available in warm core eddies. Salinity measurements are in agreement with previous surveys and show the large influence of the Amazon-Orinoco river plume (Rudzin et al., 2017).

The characteristics of these warm core eddies in the Caribbean Sea provide a framework which can be used to identify eddies during the passage of Matthew. Based on this Section, the data analysis will focus on sea surface temperature, ocean heat content and sea surface height anomalies relative to Matthew's track. This will give insight into the relation between occurrence of warm core eddies and Matthew's rapid intensification.

2.3. Influence of Warm Core Eddy on Tropical Cyclone

When a tropical cyclone passes over a warm core eddy, the cyclone-induced cooling will be reduced such that heat fluxes decrease less or even maintain/increase their magnitude. Thus the tropical cyclone can reach a larger fraction of its maximum potential intensity (Jaimes et al., 2009). In general, the warmer an ocean anomaly is, the larger the intensification relative to normal ocean conditions is.

There have been many examples of tropical cyclones rapidly intensifying in (sub)tropical areas. Some of these tropical cyclones have been analysed with respect to their rapid intensification, although such analyses are yet to be made for tropical cyclones in the Caribbean Sea. Because the Caribbean Sea shares a lot of characteristics with the Gulf of Mexico (interconnected), case studies for this area will provide useful results. Studies even show signs of connectivity between Caribbean and Gulf of Mexico warm eddies (Murphy et al., 1999; Rudzin et al., 2017).

The Gulf of Mexico is well-known for its warm core eddies, generated by separation of the Loop Current (Smith IV, 1986). Hurricane Opal of 1995 is an example where the tropical cyclone developed into a hurricane 24H before landfall. During this rapid intensification period, Opal moved over a warm core eddy. Numerical simulations indicate that the rapid intensification is largely due to an extraction of 40% of the excess heat content made available by the warm core eddy (Hong et al., 2000; Shay et al., 2000). Most of this transport of heat is achieved by surface fluxes, such as the sensible and latent heat fluxes.

Negative feedback is defined as a loop in which the cyclone-induced ocean response weakens the cyclone and in turn the weakened cyclone generates a weaker ocean response. As mentioned in Section 2.1, the presence of tropical cyclones leads to the cooling of the upper ocean layer, which is defined as the cyclone-induced ocean response. Since the tropical cyclone depends on the heat fluxes from the ocean to maintain/increase its strength, cooling will reduce this flux and in response, the tropical cyclone will weaken. The weakened tropical cyclone will then induce weaker cooling of the upper ocean. This spiral of responses will stop when either the tropical cyclone does not weaken anymore (or even dissipates) or the upper ocean layer is not cooled substantially. Hong et al. (2000) show that the negative feedback effect is stronger without the presence of a warm core eddy, indicating that tropical cyclones passing over a warm core eddy experience less influence of the ocean and thus are more eligible for rapid intensification.

A case study of Hurricanes Katrina and Rita by Jaimes et al. (2009) shows the influence of the ocean mixed layer on the intensity of tropical cyclones. The response of the tropical cyclone depends on the depth of the 26°C isotherm and thus the amount of negative feedback. As mentioned in the previous paragraph, negative feedback is known to affect the ocean mixed layer and heat fluxes in the form of upper-ocean cooling. Sea surface temperature cooling in the order of $\Delta SST > 1°C$ indicates large negative feedback and thus decreased intensity of tropical cyclones, whereas smaller or equal values hold the opposite.

Air-sea fluxes combined with negative feedback in ocean cooling significantly impact the rapid intensification of tropical cyclones. Tropical cyclone Nargis in 2008 is yet another example where 24H before landfall, the tropical cyclone rapidly intensified from a category-1 (Simpson and Saffir, 1974) to category-4 storm. Although Nargis took place in the Bay of Bengal (Indian Ocean), observations indicate that Nargis passed over a warm ocean anomaly in a similar way to the previous case studies. Lin et al. (2009) conclude that due to reduced cyclone-induced ocean cooling over a warm ocean anomaly, less negative feedback is prompted by the ocean. Because of this, more air-sea enthalpy flux is available than in normal ocean conditions. Thus, Nargis' rapid intensification occured as a result of a 300 % increase in the air-sea enthalpy flux. Without a warm ocean anomaly, this reduction in the negative feedback never happens and less enthalpy flux is available to support the rapid intensification.

The feedback system between ocean and tropical cyclone is essential in understanding rapid intensification. Figure 2 shows a summary of the feedback system in the form of a block diagram. Combined with the results of the case studies and general theory, a distinction

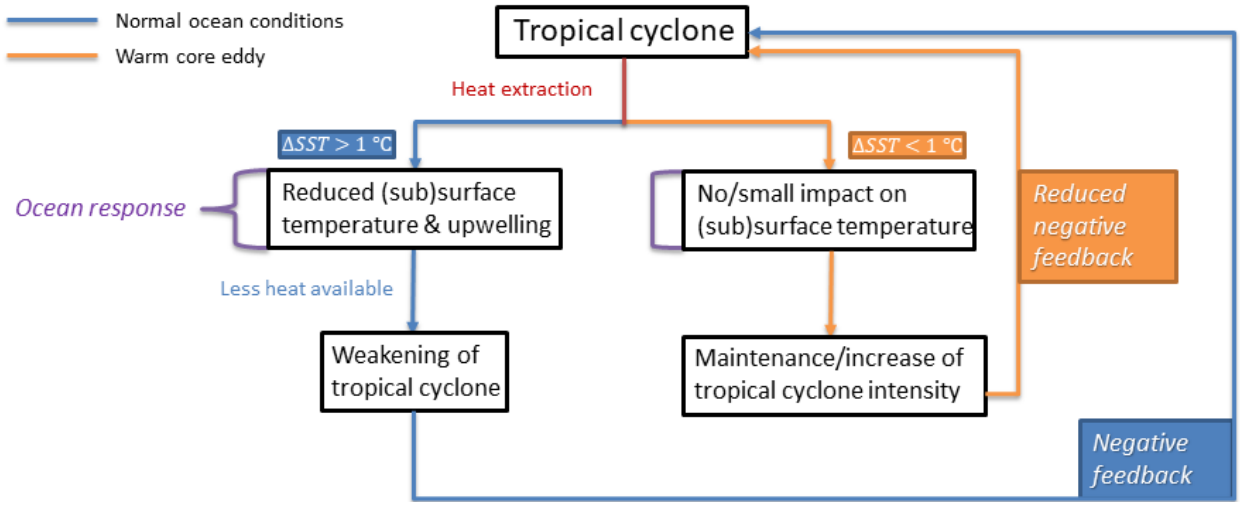

Fig. 2 *The feedback system between ocean and tropical cyclones in the form of a block diagram. The change in sea surface temperature is used as the boundary between normal ocean conditions and warm core eddies. Reduced negative feedback is not necessarily leading to the weakening of the tropical cyclone; in actuality, most observations of rapid intensification of tropical cyclones takes place when the negative feedback is reduced.*

can be made between the effect of the ocean on tropical cyclones, with and without the presence of warm core eddies.

2.4. Dataset

For this study, datasets from the Mercator global reanalysis model (Ferry et al., 2010) and ECMWF reanalysis model (Uppala et al., 2005) are used. The dataset from Mercator contains the salinity, temperature, three-dimensional northward and eastward velocity fields, sea surface height and the ocean mixed layer depth per grid cell. The ECMWF dataset contains data for the sensible and latent heat fluxes.

The temporal extent of the Mercator dataset is between 1 September and 31 October. Fluctuations are averaged per day, meaning that the temporal resolution is set at daily values. The study domain is located within the region of 80°-55° W and 8°-23° N, and the resolution in longitude and latitude is almost equal to $1/12°$. For the depth, results are given at the center of the grid cells and most grid points are located in the upper 150 m. The maximum depth is 5728 m and depth intervals are non-linearly spaced, e.g. the second, third and fourth depths are equal to 1.54, 2.65 and 3.82 m respectively. Data at the first depth (0.49 m) are presumed as sea surface values.

The ECMWF dataset contains data for the entire world calculated every 3 hours, extending from 1 September to 31 October. Based on the map domain resulting from the Mercator dataset, the ECMWF dataset is cropped to match the area of interest at approximately 80.25°-55.5° W and 8.25°-23.25° N. The spatial resolution is 0.75° in longitude and latitude.

Both datasets used in this study almost have the same spatial and temporal domain, however, there is a significant difference in the resolutions. The temporal difference can be solved by averaging the ECMWF dataset per day. The spatial resolution is much finer for the Mercator dataset, thus spatial averaging would lead to loss of detailed information. Therefore, study parameters will be exclusively extracted from the Mercator dataset except for parameters that are missing but present in the ECMWF dataset.

For the data analysis, the ocean heat content is not provided in the datasets. Therefore, Equation 1 is simplified into the following equation:

$$H = \sum_{k=1}^{n} \Delta T_k \Delta d_k \tag{2}$$

where H is the amount of ocean heat content [$°Cm$] and ΔT_k and Δd_k the difference in temperature and depth respectively between layers in the data set. As can be seen from the units, H has been simplified by neglecting the density and specific heat of water, since they are assumed to be constant spatially and temporally in the area of interest.

3. Results & Discussion

In this Section, the results of the data analysis will be shown and discussed according to the knowledge provided by Section 2. Sea surface height (Section 3.1), sea surface velocity (Section 3.2) and (sea surface) temperature (Section 3.3) are analysed to assess if a warm core eddy is present. Ocean heat content and surface heat fluxes will be analysed with respect to the transport of heat between the ocean and Matthew (Section 3.4). In the Appendices, more results are shown.

3.1. Sea surface height

Tropical cyclone Matthew's positions are known from 28 September till 10 October Stewart (2017). Warm core eddies were identified by observing the sea surface height for positive anomalies. Figure 3 shows the sea surface height of the Caribbean Sea 1 day before Matthews rapid intensification.

As can be seen in Figure 3, a positive anomaly is observed at coordinates (67° W, 14.2° N) in the path of Matthew (also pointed out by the red arrow). The sea surface height at this location, when averaged spatially over the anomaly according to the contour level, is approximately 0.29 m. The minimum and maximum sea surface heights, within is this anomaly, are approximately 0.26 and 0.32 m respectively. According to theory and observations (Section 2.2), these results indicate a warm core eddy just before the rapid intensification of Matthew. The spatial scale is not in accordance to observations, since the diameter of this anomaly is about 100 km (based on Figure 3), whereas observations and numerical simulations show results larger than 200 km. However, eddies grow in diameter when propagating westwards in the Caribbean Sea, but this can't be checked with the current dataset due to the limitation in the temporal extent. The warm core eddies observed at coordinates (73° W, 16° N) and (77.5° W, 15.5° N) are much more distinct in spatial scale and they show a larger sea surface height.

The sea surface height difference between the beginning and ending of the rapid intensification period was also analysed. Figure 4 specifies this mapped difference, showing a large decrease in sea surface height at the location of rapid intensification. This could indicate that due to Matthews extraction of heat, the warm core eddy loses its strength and therefore the vertical expansion of the warmer water is reduced and the eddy shrinks in size.

3.2. Sea surface velocity

The sea surface height map does not indicate clearly the existence of a warm core eddy at the time Matthew rapidly intensified. The next step was the analysis of the surface velocities. Since a rotational flow exists in a warm core eddy, surface velocities should also show a rotational velocity field. The results are shown in Figure 5 for the whole area. Figure 6 shows the zoomed map of the location of the suspect warm core eddy.

The positive anomaly that was observed at coordinates (67° W, 14.2° N) according to the sea surface height is not visible in the velocity field. More specifically, the arrows in the velocity field at this location do not indicate a rotational flow, whereas the more distinct eddies show this effect. A possible explanation could be the dominance of the Caribbean Current over the eddy rotational velocities. Observational studies show that the Caribbean Current has a mean flow of approximately 100 cm/s and eddy swirl velocities are in the order of 40 cm/s (Richardson, 2005). The Caribbean Current flows westwards and this means that in presence of a warm core eddy, the westward velocities at the northern side of the eddy would be reduced more relative to the westward velocities at the southern side. This can be observed with the red boxes in Figure 6.

3.3. Temperature

Results from the previous sections do provide evidence to conclude the presence of a warm core eddy at the location of rapid intensification of Matthew, although small in size and weak. The data analysis of the temperature profiles were thus evaluated to identify a substantial difference of sea surface temperature at the presumed location of the warm core eddy. Figure 7 shows the sea surface temperature at 29 September, before rapid intensification.

A warm anomaly is approximately found at coordinates (67° W, 13.8° N). The position however doesn't fully match the location of the anomaly of the sea surface height. It is however remarkable that both analyses show anomalies close by and this could indicate a certain spatial difference between the cores of the sea surface height and temperature. Moreover, sea surface temperatures decrease significantly after Matthews passage, showing the extent of the upwelling caused by Matthew (see Appendix B). Figure 8 shows a close up of the warm ocean anomaly.

The warm anomaly, when spatially averaged over its extent, has a temperature of 29.7 $^{\circ}C$ with minimum and

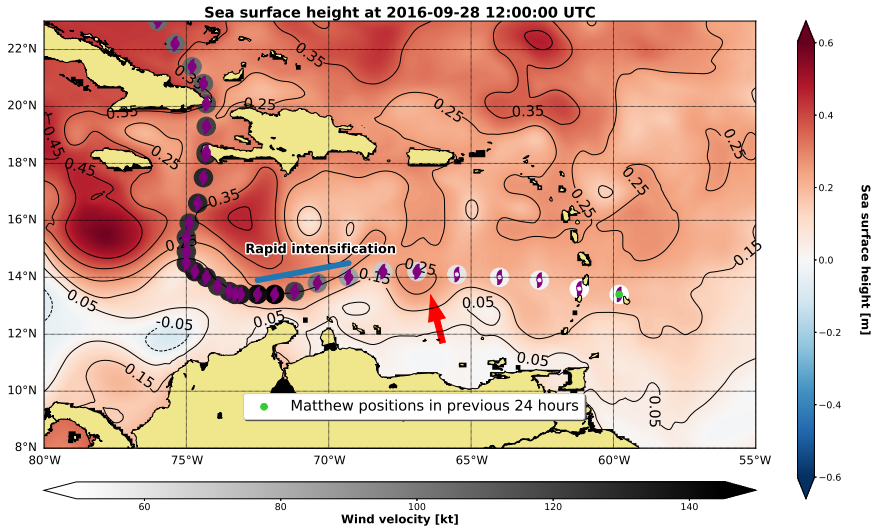

Fig. 3 *Map of sea surface height at 29-09-2016. Contour interval is 0.1 m between -0.35 and 0.45 m. The rapid intensification period between 30-01 and 01-10 is shown with the blue line. All of Matthews positions are shown with the colored circles, whereas Matthews current position or positions in the previous 24H are shown with the green dots. The colors of the circles indicate the strength of the wind velocity, defined in [kt] according to data from Stewart (2017). The colorbar on the right hand side shows the magnitude of the sea surface height, whereas the colorbar underneath the figures shows the magnitude of the wind velocity. Official tropical storm symbols are used inside the colored circles to indicate the storm category of Matthew: the open symbol means that Matthew is in a 'tropical cyclone' state whereas the closed symbol means that Matthew is in a 'hurricane' state.*

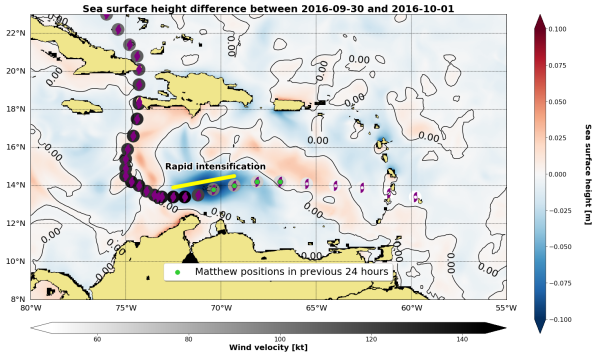

Fig. 4 *The difference in sea surface height between 30-09-2016 and 01-10-2016. For more information about figure symbols, reference is made to Figure 3.*

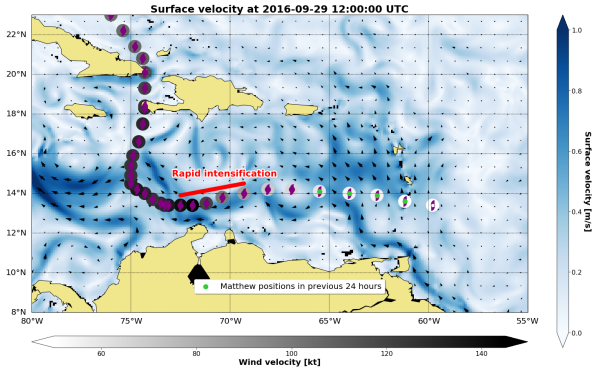

Fig. 5 *Map of surface velocity at 29-09-2016. The arrows indicate the direction of the surface velocity and the colors show the magnitude in [m/s]. For more information about figure symbols, reference is made to Figure 3.*

maximum temperatures of 29.4 and 30.1 $°C$. According to the general physical mechanisms, the sea surface temperature at this location should be reduced considerably due to mixing and upwelling (Section 2.3). The temperature at 30 September at the exact same location shows an spatially averaged value of 29.4 $°C$ (not shown), indicating that the negative feedback provided by the ocean on the tropical cyclone is almost negligible. As a result, Matthew could potentially intensify further, which the tropical cyclone certainly did by rapidly intensifying two days after passing over this warm anomaly.

The vertical structure of the temperature at the warm anomaly location was analysed to look at the changes in time. Results are shown in Figure 9. The passage of a warm core eddy would result in the deepening of the isotherms over a certain time. This can be calculated with the eddy propagation velocity and its diameter. If e.g. the eddy propagation velocity of 12 cm/s is assumed (Section 2.2), a daily propagation velocity of

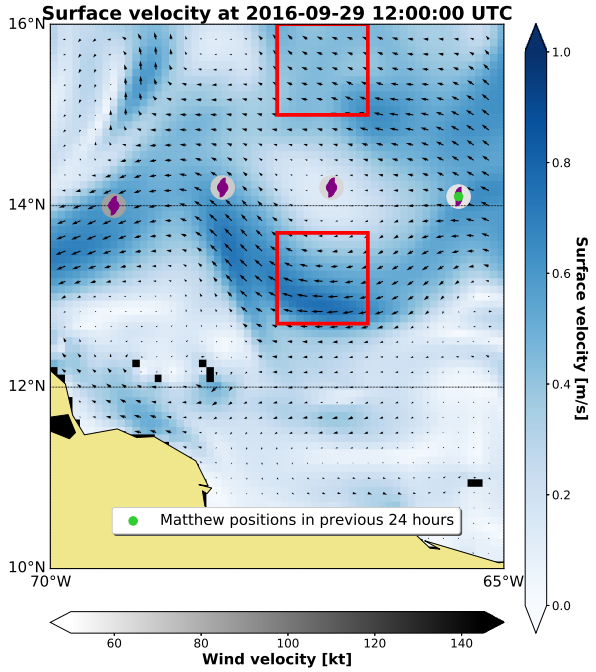

Fig. 6 *Zoomed map of location (supposed) eddy for the surface velocity at 29-09-2016. The arrows indicate the direction of the surface velocity and the colors show the magnitude in $[m/s]$. For more information about figure symbols, reference is made to Figure 3.*

10.4 *km* is calculated. Assuming a diameter of 100 *km*, the eddy should pass over a point in approximately 10 days. When the tropical cyclone extracts heat from the eddy, it weakens in strength but this does not necessarily conclude in a decrease/increase of the eddy propagation velocity since this is highly dependent on background currents.

It is clear from Figure 9 that the vertical temperature profile shows decreased values after the passage of Matthew around 30 September. The isotherms move to smaller depths and this is in line with theory, since Matthew will induce upwelling, causing the rise of colder waters in the upper ocean layer. There is also reasonable evidence for the presence of a warm core eddy, since the isotherms decrease with depth in time. Assuming that the core of the eddy passes over this point on 29 September (relative to 10 days deepest isotherm points), it is obvious that after this date the temperatures will decrease. It is however quite odd that the temperature between 1 and 3 October seems to rise at all depths, since the combined effect of the passage of the eddy and heat extraction by Matthew should result in a monotonically decreasing temperature profile. Other sources of heat may be responsible for this sudden increase in temperature, of which the Amazon-Orinoco river plume seems the most plausible.

On the time scale of approximately 20 days, the rise and fall of the temperature can be seen. The blue lines in Figure 9 indicate the points at which the gradients of the isotherms are almost equal to zero, which means that the temperature is constant. The pattern again resembles the changes in temperature over 10 days, but the time scale is much larger. In order to assess this more accurately, propagation velocities at the location of the anomaly should be calculated more accurately.

The vertical temperature profiles in Figure 10 show the difference of the temperature before and after Matthew's passage. The temperature decreases several tenths of a degree in one day, showing the extent of the heat extraction by Matthew. It is surprising that the temperature profiles at 21 September and 21 October do not match at all. This could be due to Matthew, however, other physical phenomena on large time scales can be of influence.

3.4. Ocean heat content and surface heat fluxes

The last step in the data analysis involved the ocean heat content at the expected location of the warm core eddy. The ocean heat content is approached with Equation 2 for 36 layers in the three-dimensional grid. This results in a maximum depth equivalent to approximately 155 *m*, which indicates that only the ocean heat content of the upper ocean layer is examined. This depth is based on further analysis, shown in Figure 10, where it was found that at deeper depths than this value, temperature changes in time were negligible.

As the theory of Section 2.2 stated, warm core eddies have more ocean heat content available, which can be transferred by surface heat fluxes to tropical cyclones that are passing over. The upper ocean heat content is shown in Figure 11a. Before rapid intensification, Matthew clearly passes over an area with relatively high ocean heat content. The change of ocean heat content is shown in Figure 11b. Matthew clearly extracts heat from the ocean at the time it intensifies.

These results show that a warm ocean anomaly must be present since the ocean heat content at the location before rapid intensification is larger than in other parts of the Caribbean Sea. The heat from the ocean is transferred to the tropical cyclone by surface heat fluxes. Surface heat fluxes are therefore important, since they indicate the amount of negative feedback in the system.

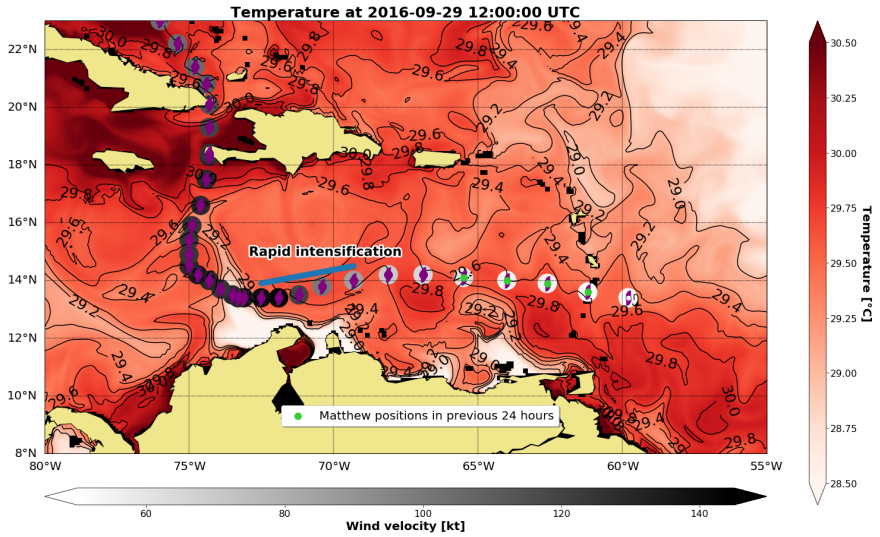

Fig. 7 *Map of sea surface temperature at 29-09-2016. Contour interval is 0.2 °C between 29 and 30 °C. The colors indicate the magnitude of the sea surface temperature and the colorbar on the right hand side provides the values. For more information about figure symbols, reference is made to Figure 3.*

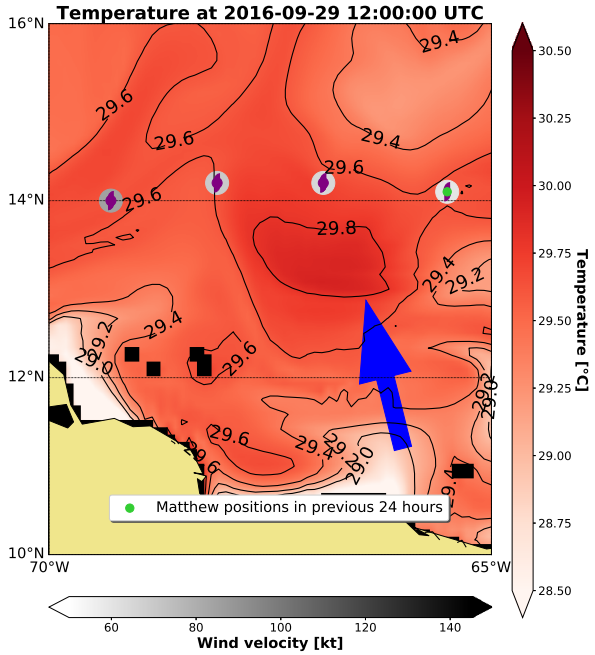

Fig. 8 *Sea surface temperature zoomed on warm ocean anomaly (67° W, 13.75° N).*

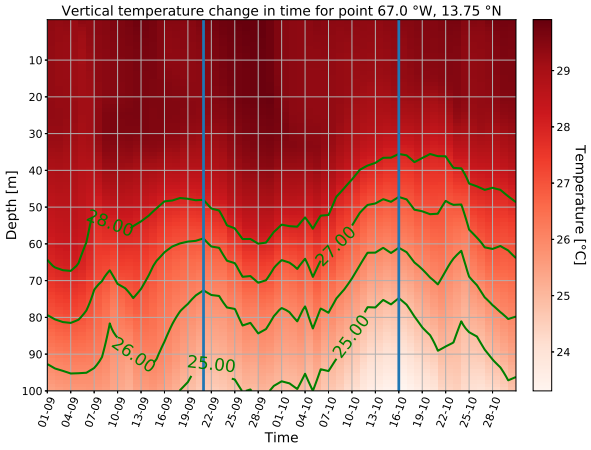

Fig. 9 *Vertical temperature profile in time between 01-09 and 31-10 at coordinates (67° W, 13.75° N). The green lines show the 25°C, 26°C, 27°C and 28°C isotherms.*

When there is significant upper ocean cooling by the cyclone, surface heat fluxes will be small. If the upper ocean cooling is negligible due to the presence of a warm anomaly, the opposite case holds ans heat fluxes will not be affected.

Surface heat fluxes between 29-09 and 01-10 are shown in Figure 12. More specifically, enthalpy fluxes are shown in these subfigures. The enthalpy flux is a summation of the sensible and latent heat fluxes. As was observed in previous studies (Lin et al., 2009), the latent heat flux is the main contributor to the enthalpy flux. The enthalpy flux before and during rapid intensification show a significant transport of heat to feed Matthew for its strengthening. Remarkable is the shift in the enthalpy flux during the rapid intensification period (Figure 12b) to the north of Matthews track. Matthew's di-

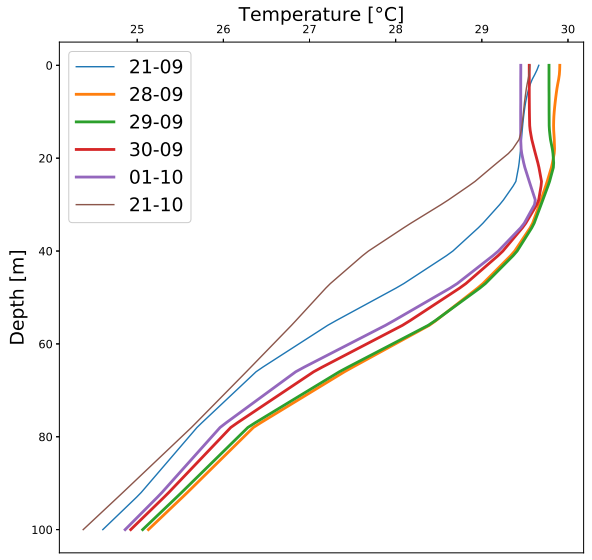

Fig. 10 *Temperature profile for different time steps at coordinates (67° W, 13.75° N).*

ameter is large enough to cover the Caribbean Sea in latitude and results indicate that heat extraction is not automatically near the eye of the tropical cyclone.

Further analysis with surface fluxes is recommended, where instead of averaged values per day, hourly values would provide more information on the rapid intensification of Matthew. Precise time intervals can be distinguished and the difference between the sensible and latent heat fluxes can be assessed more accurately.

4. Conclusion & Recommendations

Based on the results from the previous Section, conclusions and further recommendations are given in this Section.

This study started with the following research question:

Does the rapid intensification period of Hurricane Matthew coincide with Warm Core Eddies in the Caribbean Sea?

The results show some indications of the presence of a warm core eddy. There is a positive sea surface height anomaly just before the rapid intensification of Matthew took place. There was also a warm anomaly present in the track and the shape and location of this anomaly matched the sea surface height anomaly very

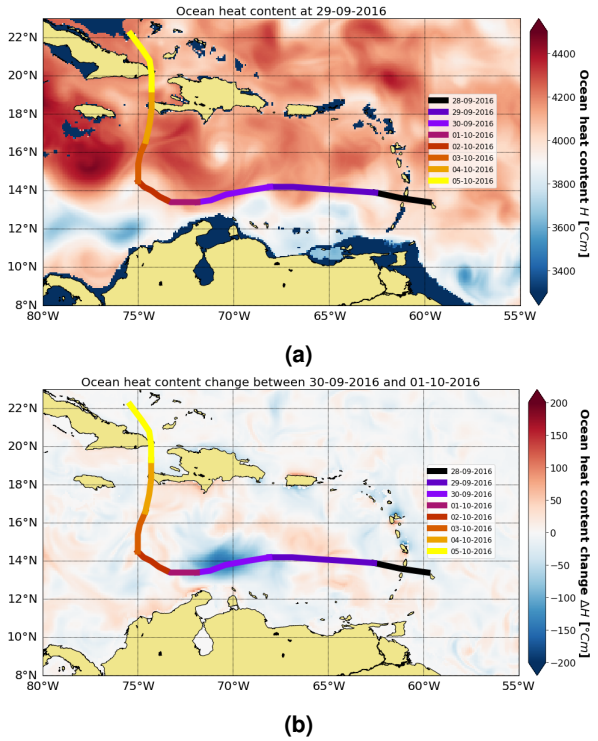

Fig. 11 *(a) and (b): Maps of ocean heat content at 29-09-2016 and ocean heat content change between 30-09 and 01-10. The colored map shows the magnitude of the ocean heat content, whereas the colorbar on the right hand side provides values. The colored lines indicate Matthews path during a particular day. Rapid intensification took place between 30-09 and 01-10.*

good. However, surface velocities do not indicate a rotational flow, which is certainly a characteristic of eddies. This means that either a warm core eddy was not present or the eddy was masked due to the stronger background flow (Caribbean Current).

The vertical temperature profile at the supposed location of the eddy shows signs of a warm core eddy. The 26°C isotherm layer depth does change substantially in time after Matthew's passage, but on a longer time scale, the same effect is found and this could indicate the presence of a much larger physical mechanism.

The ocean heat content shows that there was relatively more heat available before rapid intensification took place. This is also seen in the daily ocean heat content change, showing that Matthew extracted this heat to intensify. However, this result does not necessarily lead to evidence for the presence of a warm core eddy. The most important question should be on why there is more ocean heat content available, excluding warm core

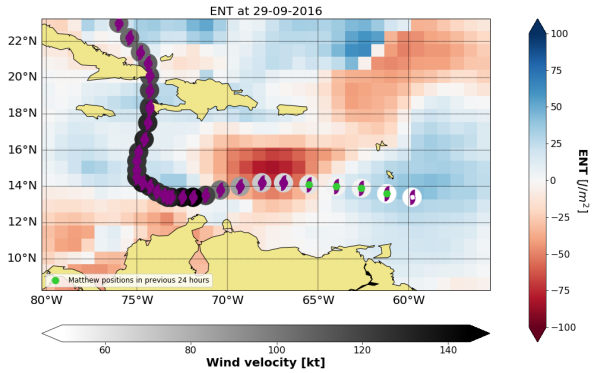

(a) *Map of enthalpy flux at 29-09-2016*

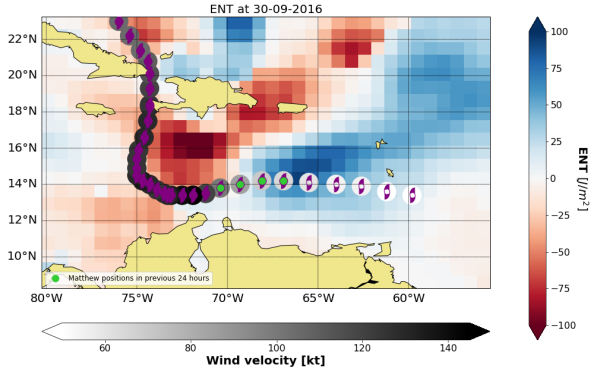

(b) *Map of enthalpy flux at 30-09-2016*

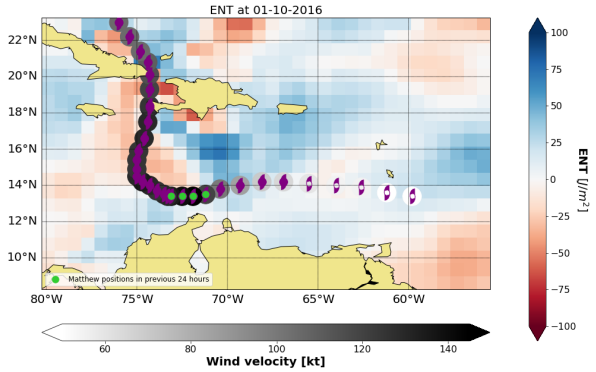

(c) *Map of enthalpy flux at 01-10-2016*

Fig. 12 *Maps of enthalpy fluxes between 29/09-01/10. The downward fluxes are positive and upward fluxes are negative. For more information about figure symbols, reference is made to Figure 3.*

eddies since previous results do not fully support their presence.

Surface heat fluxes are the main transport mechanisms of heat between ocean and tropical cyclone. The results show that during rapid intensification, surface heat fluxes were most prominent north of Matthew. This

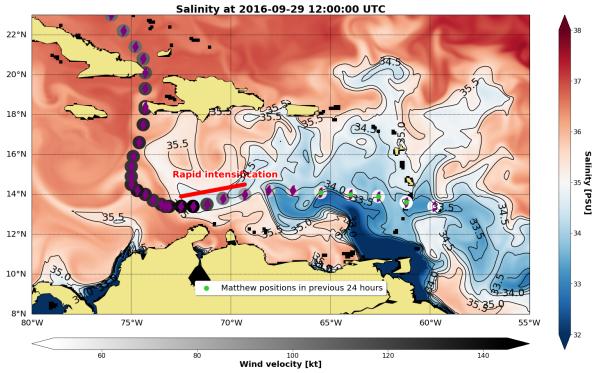

Fig. 13 *Map of salinity at 29-09-2016. Contour interval is 0.5 PS U between 33 and 36 PS U. For more information about figure symbols, reference is made to Figure 3.*

shows that the location of heat extraction and feeding of a tropical cyclone is most certainly not linked to the eye of the tropical cyclone. Future research should therefore be cautious to include the whole area affected by the tropical cyclone, not limiting their view to the eye/centre of the tropical cyclone.

Further recommendations are summarized in the following list:

- The evidence provided by the surface velocities is not in line with sea surface height and sea surface temperature. The reason for this might be due to the strong Caribbean Current overriding the swirl velocities of the eddy, effectively hiding it behind the surface flow. Numerical simulations can help to identify the relation between the magnitude of these velocities and whether the eddy is hidden by this flow.

- Sea surface salinity as a measure for eddies in the Caribbean Sea is not a good approach, as was found by Rudzin et al. (2017). This is due to the influence of the Amazon-Orinoco river plume, discharging fresher and warmer water in the Caribbean Sea. The location of the sea surface temperature and sea surface salinity (Figure 13) anomalies match very good, indicating that not a warm core eddy but the river plume might be responsible for the rapid intensification of Matthew.

  Reul et al. (2014) show that due to the Amazon-Orinoco river plume, tropical cyclone induced upper ocean cooling is reduced by 50% over waters affected by the river plume relative to open ocean water. This could be another reason, not related to the presence of a warm core eddy, why Matthew

rapidly intensified. Numerical simulations could show the difference between tropical cyclone intensification with and without the river plume.

- One possible explanation for the rapid intensification of Matthew could be related to La Niña. Although this is a phenomenon on a much larger scale, the influence of La Niña actually leads to more hurricanes and tropical cyclones in the area around the Caribbean Sea. This is due to the weakened vertical wind shear and weakened atmospheric stability (Bell and Chelliah, 2006). The amount of tropical cyclones increases, but it is unknown if the (average) strength of the tropical cyclones is also higher during La Niña. Further studies, preferably with numerical models, are recommended.

References

Andrade, C. A., Barton, E. D., 2000. Eddy development and motion in the Caribbean Sea. Journal of Geophysical Research: Oceans 105 (C11), 26191–26201.

Bell, G. D., Chelliah, M., 2006. Leading tropical modes associated with interannual and multidecadal fluctuations in North Atlantic hurricane activity. Journal of Climate 19 (4), 590–612.

Blake, E., Gibney, E., Brown, D., Mainelli, M., Franklin, J., Kimberlain, T., Hammer, G., 2008. Tropical Cyclones of the Eastern North Pacific Ocean, 1949-2006. In: 28th Conference on Hurricanes and Tropical Meteorology.

Blake, E. S., Rappaport, E. N., Jarrell, J. D., Landsea, C., Center, T. P., 2007. The deadliest, costliest, and most intense United States tropical cyclones from 1851 to 2006 (and other frequently requested hurricane facts). NOAA/National Weather Service, National Centers for Environmental Prediction, National Hurricane Center Miami.

Blake, E. S., et al., 2018. The Deadliest, Costliest, and Most Intense United States Tropical Cyclones from 1851 to 2010 (and Other Frequently Requested Hurricane Facts). Tech. rep., National Hurricane Center.

Carton, J. A., et al., 1999. Caribbean Sea eddies inferred from TOPEX/Poseidon altimetry and a 1/6 Atlantic Ocean model simulation. Journal of Geophysical Research: Oceans 104 (C4), 7743–7752.

Corredor, J. E., Morell, J. M., Lopez, J. M., Capella, J. E., Armstrong, R. A., 2011. Cyclonic eddy entrains Orinoco River Plume in eastern Caribbean. Eos, Transactions American Geophysical Union 85 (20), 197–202.
URL `https://agupubs.onlinelibrary.wiley.com/doi/abs/10.1029/2004EO200001`

Creel, L., 2003. Ripple effects: population and coastal regions. Population Reference Bureau Washington, DC.

Emanuel, K. A., 1986. An air-sea interaction theory for tropical cyclones. Part i: Steady-state maintenance. Journal of the Atmospheric Sciences 43 (6), 585–605.

Ferry, N., Parent, L., Garric, G., Barnier, B., Jourdain, N. C., et al., 2010. Mercator global Eddy permitting ocean reanalysis GLORYS1V1: Description and results. Mercator-Ocean Quarterly Newsletter 36, 15–27.

Goldenberg, S. B., Landsea, C. W., Mestas-Nuñez, A. M., Gray, W. M., 2001. The recent increase in Atlantic hurricane activity: Causes and implications. Science 293 (5529), 474–479.

Holland, G., 1993. Ready Reckoner—Chapter 9, Global guide to tropical cyclone forecasting, WMO. TC (560).

Holland, W. R., Lin, L. B., 1975. On the generation of mesoscale eddies and their contribution to the oceanicgeneral circulation. i. a preliminary numerical experiment. Journal of Physical Oceanography 5 (4), 642–657.

Holliday, C. R., Thompson, A. H., 1979. Climatological characteristics of rapidly intensifying typhoons. Monthly Weather Review 107 (8), 1022–1034.

Hong, X., Chang, S. W., Raman, S., Shay, L. K., Hodur, R., 2000. The interaction between Hurricane Opal (1995) and a warm core ring in the Gulf of Mexico. Monthly Weather Review 128 (5), 1347–1365.

Jaimes, B., et al., 2009. Mixed layer cooling in mesoscale oceanic eddies during Hurricanes Katrina and Rita. Monthly Weather Review 137 (12), 4188–4207.

Jouanno, J., Sheinbaum, J., Barnier, B., Molines, J.-M., Debreu, L., Lemarié, F., 2008. The mesoscale variability in the Caribbean Sea. Part I: Simulations and characteristics with an embedded model. Ocean Modelling 23 (3-4), 82–101.

Kaplan, J., DeMaria, M., 2003. Large-scale characteristics of rapidly intensifying tropical cyclones in the north atlantic basin. Weather and forecasting 18 (6), 1093–1108.

Kaplan, J., DeMaria, M., Knaff, J. A., 2010. A revised tropical cyclone rapid intensification index for the Atlantic and eastern North Pacific basins. Weather and forecasting 25 (1), 220–241.

Lin, I.-I., et al., 2009. Warm ocean anomaly, air sea fluxes, and the rapid intensification of tropical cyclone Nargis (2008). Geophysical Research Letters 36 (3).

Lobel, P., Robinson, A., 1986. Transport and entrapment of fish larvae by ocean mesoscale eddies and currents in Hawaiian waters. Deep Sea Research Part A. Oceanographic Research Papers 33 (4), 483–500.

Malmstadt, J., Scheitlin, K., Elsner, J., 2009. Florida hurricanes and damage costs. southeastern geographer 49 (2), 108–131.

Molinari, R. L., Spillane, M., Brooks, I., Atwood, D., Duckett, C., 1981. Surface currents in the Caribbean Sea as deduced from Lagrangian observations. Journal of Geophysical Research: Oceans 86 (C7), 6537–6542.

Murphy, S. J., Hurlburt, H. E., O'Brien, J. J., 1999. The connectivity of eddy variability in the Caribbean sea, the Gulf of mexico, and the Atlantic Ocean. Journal of Geophysical Research: Oceans 104 (C1), 1431–1453.

Pielke Jr, R. A., Gratz, J., Landsea, C. W., Collins, D., Saunders, M. A., Musulin, R., 2008. Normalized hurricane damage in the United States: 1900–2005. Natural Hazards Review 9 (1), 29–42.

Reul, N., Quilfen, Y., Chapron, B., Fournier, S., Kudryavtsev, V., Sabia, R., 2014. Multisensor observations of the Amazon-Orinoco river plume interactions with hurricanes. Journal of Geophysical Research: Oceans 119 (12), 8271–8295.

Richardson, P. L., 2005. Caribbean Current and eddies as observed by surface drifters. Deep Sea Research Part II: Topical Studies in Oceanography 52 (3-4), 429–463.

Rudzin, J., Shay, L., Jaimes, B., Brewster, J., 2017. Upper ocean observations in eastern Caribbean Sea reveal barrier layer within a warm core eddy. Journal of Geophysical Research: Oceans 122 (2), 1057–1071.

Shay, L. K., Goni, G. J., Black, P. G., 2000. Effects of a warm oceanic feature on Hurricane Opal. Monthly Weather Review 128 (5), 1366–1383.

Simpson, R. H., Saffir, H., 1974. The hurricane disaster potential scale. Weatherwise 27 (8), 169.

Smith IV, D. C., 1986. A numerical study of Loop Current eddy inter-

action with topography in the western Gulf of Mexico. Journal of physical Oceanography 16 (7), 1260–1272.

Stewart, S. R., 2017. HURRICANE MATTHEW. Tech. rep., National Hurricane Center.

Uppala, S. M., Kållberg, P., Simmons, A., Andrae, U., Bechtold, V. d., Fiorino, M., Gibson, J., Haseler, J., Hernandez, A., Kelly, G., et al., 2005. The ERA-40 re-analysis. Quarterly Journal of the royal meteorological society 131 (612), 2961–3012.

van der Boog, C. G., 2018. The Influence of Localized Wind Stress on Eddies in the Caribbean Sea. Vol. EGU General Assembly 2018. EGU.

Appendix A. Sea Surface Height

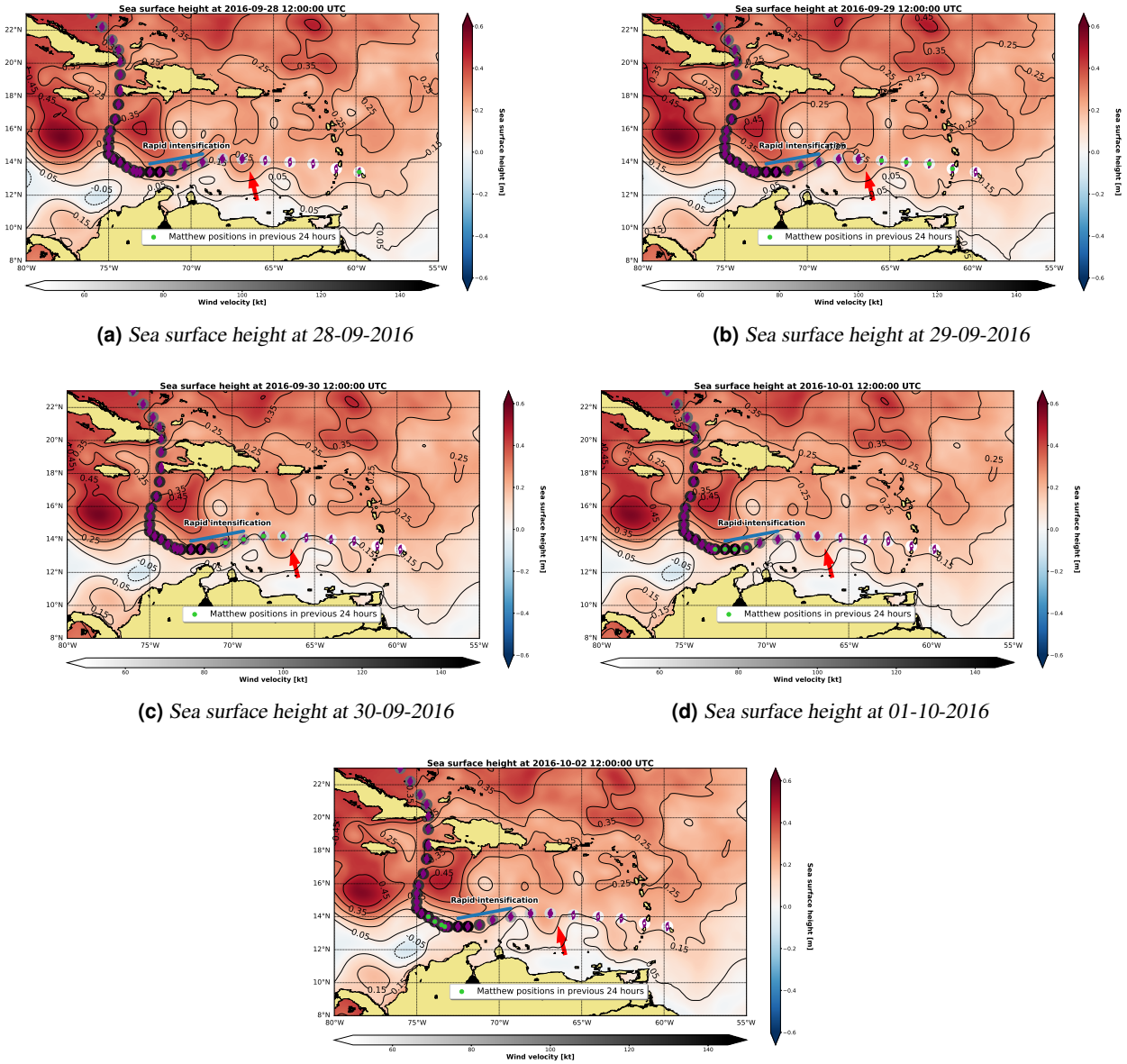

(a) *Sea surface height at 28-09-2016*

(b) *Sea surface height at 29-09-2016*

(c) *Sea surface height at 30-09-2016*

(d) *Sea surface height at 01-10-2016*

(e) *Sea surface height at 02-10-2016*

Fig. A.1 *Maps of sea surface height between 28-09 and 02-10.*

Appendix B. Sea Surface Temperature

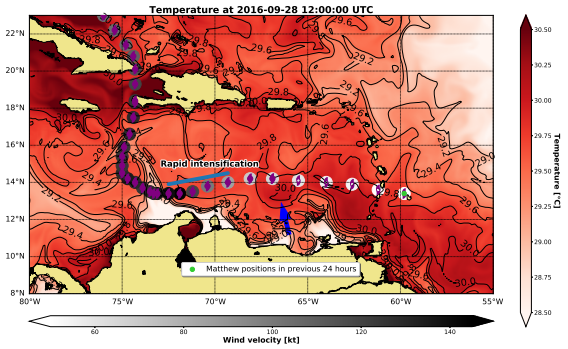

(a) *Sea surface temperature at 28-09-2016*

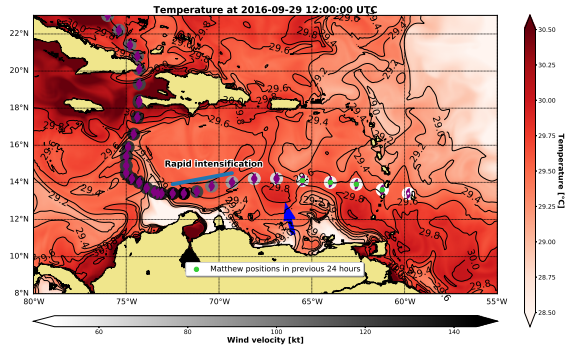

(b) *Sea surface temperature at 29-09-2016*

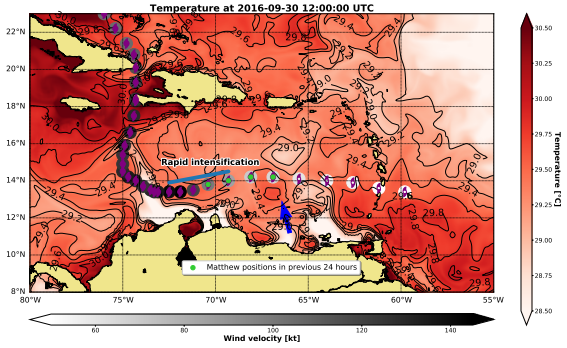

(c) *Sea surface temperature at 30-09-2016*

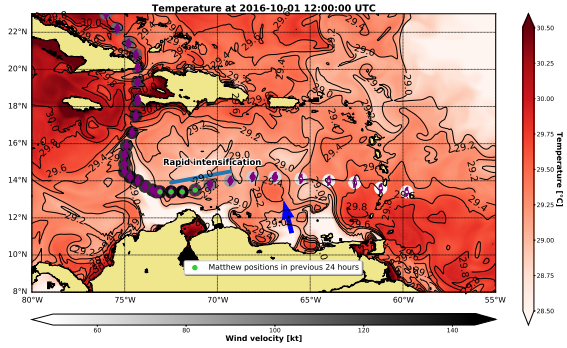

(d) *Sea surface temperature at 01-10-2016*

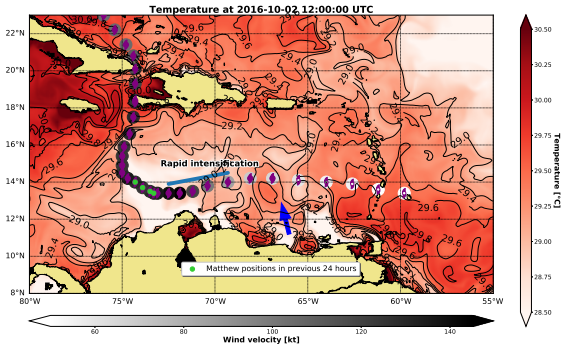

(e) *Sea surface temperature at 02-10-2016*

Fig. B.1 *Maps of sea surface temperature between 28-09 and 02-10.*

Appendix C. Sea Surface Salinity

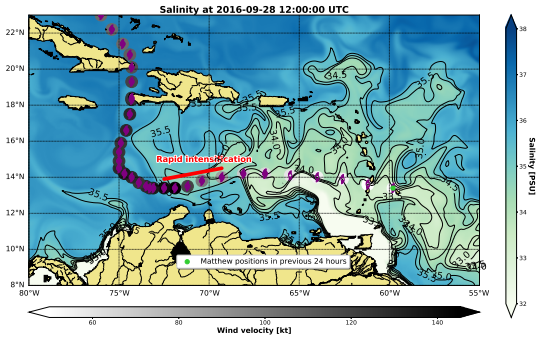

(a) *Sea surface salinity at 28-09-2016*

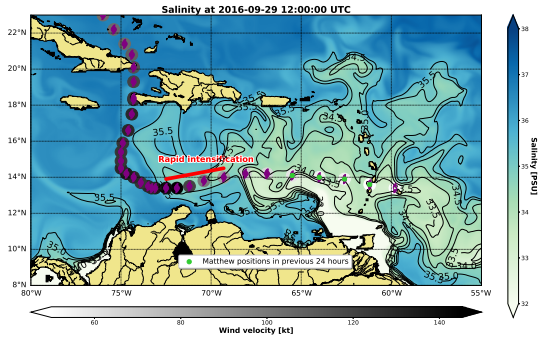

(b) *Sea surface salinity at 29-09-2016*

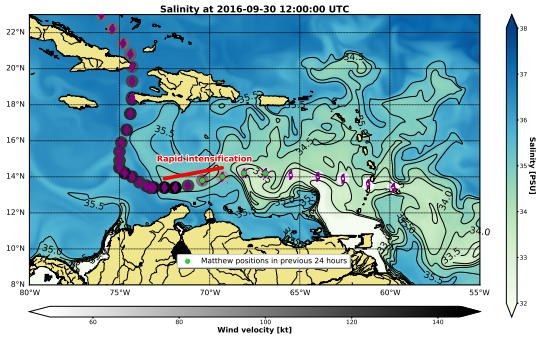

(c) *Sea surface salinity at 30-09-2016*

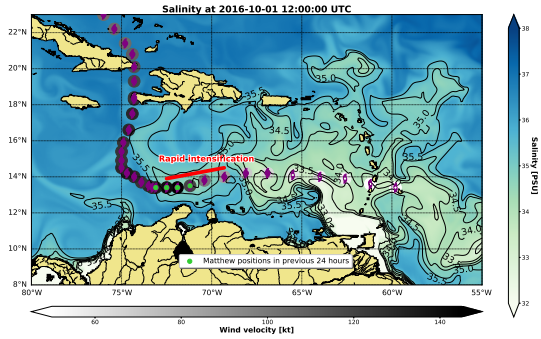

(d) *Sea surface salinity at 01-10-2016*

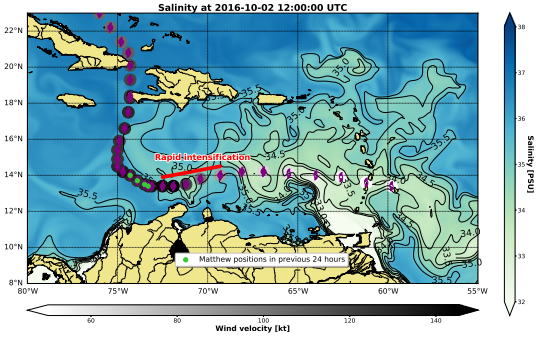

(e) *Sea surface salinity at 02-10-2016*

Fig. C.1 *Maps of sea surface salinity between 28-09 and 02-10.*

Appendix D. Ocean Heat Content

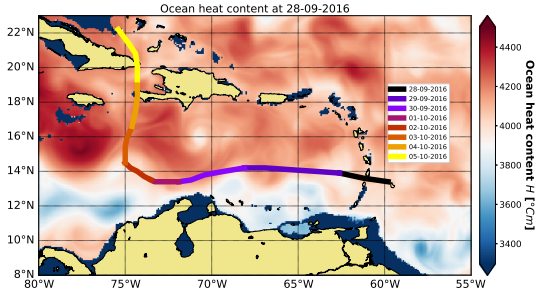

(a) *Ocean heat content at 28-09-2016*

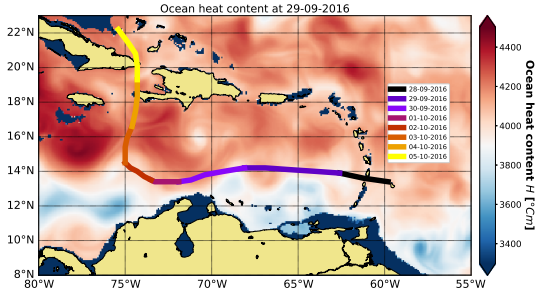

(b) *Ocean heat content at 29-09-2016*

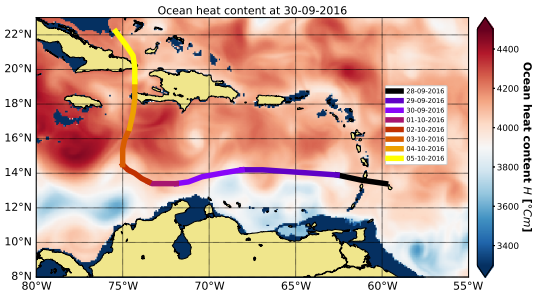

(c) *Ocean heat content at 30-09-2016*

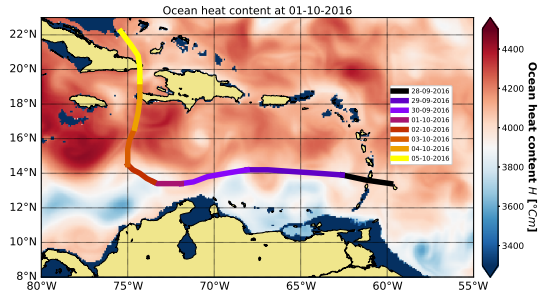

(d) *Ocean heat content at 01-10-2016*

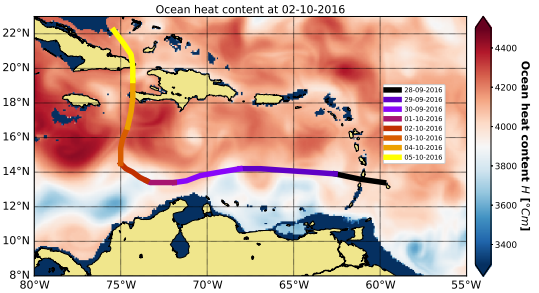

(e) *Ocean heat content at 02-10-2016*

Fig. D.1 *Maps of ocean heat content between 28-09 and 02-10.*

Appendix E. Daily Ocean Heat Content Change

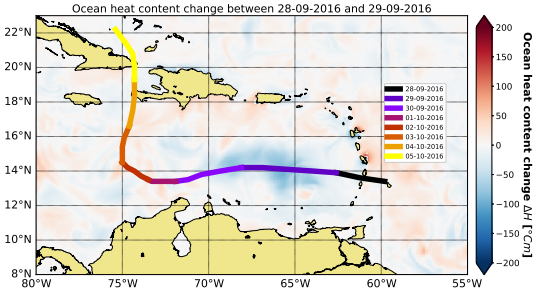

(a) *Ocean heat content change between 28-09-2016 and 29-09-2016*

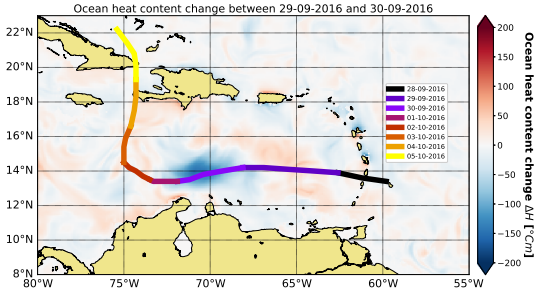

(b) *Ocean heat content change between 29-09-2016 and 30-09-2016*

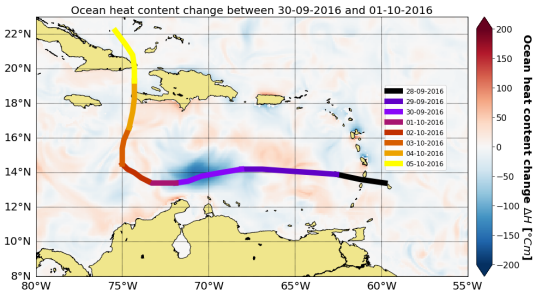

(c) *Ocean heat content change between 30-09-2016 and 01-10-2016*

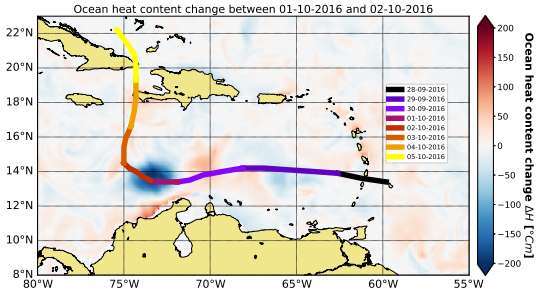

(d) *Ocean heat content change between 01-10-2016 and 02-10-2016*

Fig. E.1 *Maps of ocean heat content change between 28-09 and 02-10.*

Appendix F. Latent Heat Flux

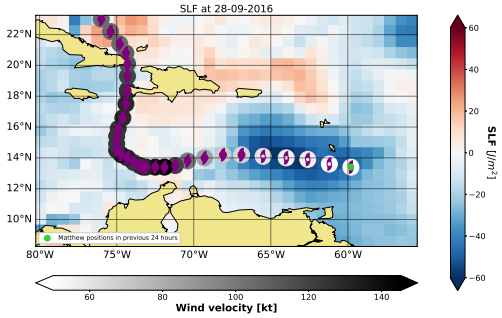

(a) *Surface latent heat flux at 28-09-2016*

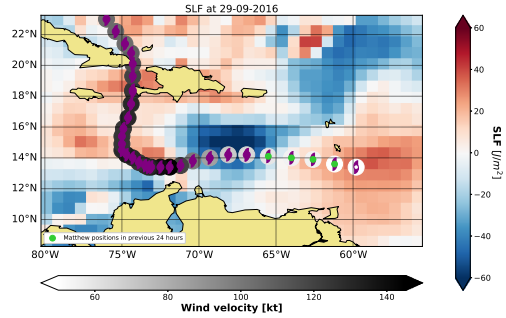

(b) *Surface latent heat flux at 29-09-2016*

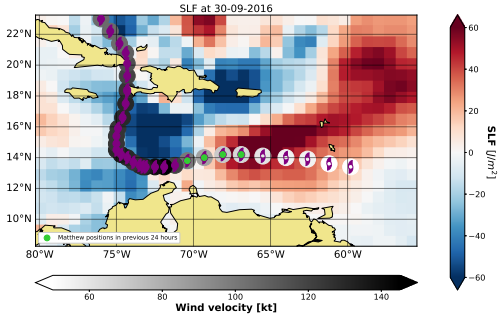

(c) *Surface latent heat flux at 30-09-2016*

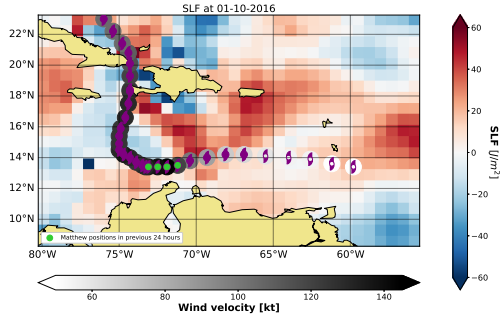

(d) *Surface latent heat flux at 01-10-2016*

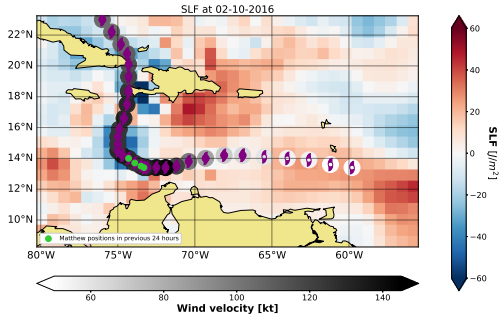

(e) *Surface latent heat flux at 02-10-2016*

Fig. F.1 *Maps of surface latent heat flux between 28-09 and 02-10.*

Appendix G. Sensible Heat Flux

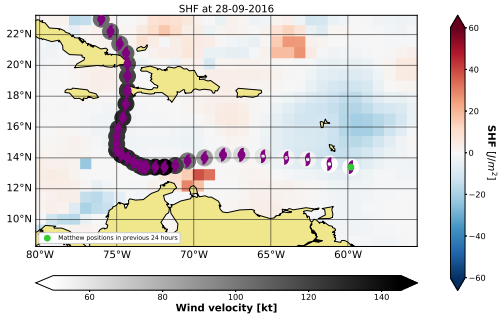

(a) *Surface sensible heat flux at 28-09-2016*

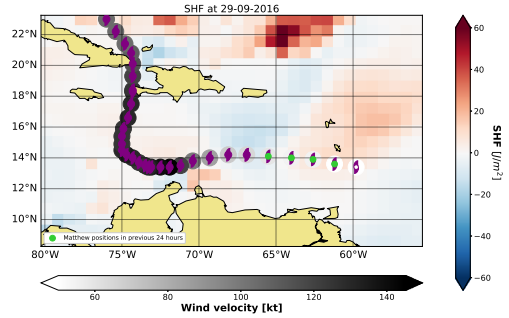

(b) *Surface sensible heat flux at 29-09-2016*

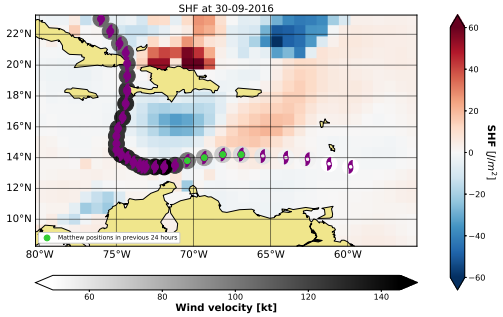

(c) *Surface sensible heat flux at 30-09-2016*

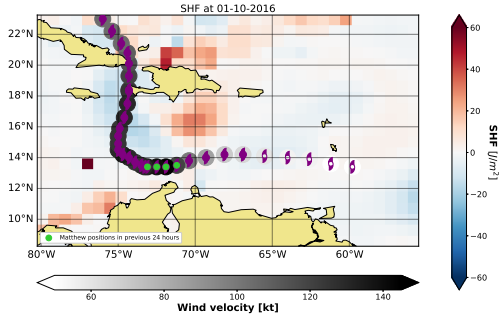

(d) *Surface sensible heat flux at 01-10-2016*

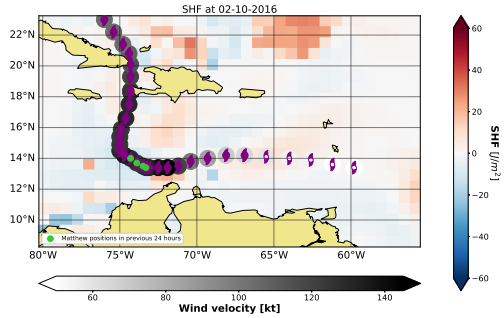

(e) *Surface sensible heat flux at 02-10-2016*

Fig. G.1 *Maps of surface sensible heat flux between 28-09 and 02-10.*